THE UNIVERSITY OF MICHIGAN

INDUSTRY PROGRAM OF THE COLLEGE OF ENGINEERING

TORSION OF STRUCTURAL SHAPES

I. A. ElDarwish
Bruce G. Johnston

March, 1964

IP-664

ensn
UMR0808

TABLE OF CONTENTS

LIST OF TABLES

LIST OF FIGURES

INTRODUCTION

The torsion constant "J" and the shear stresses due to torsion, as covered herein for certain structural sections, relate to what is often referred to as "St. Venant Torsion,"[1] which involves certain conditions, as follows. The structural shape is uniform in cross-section and the torsional moment is applied by means of opposed couples at each end in such a way that there is no restraint against longitudinal displacement at any point on the end sections. The angle of twist per unit length "θ" is thus uniform. If z is taken as the coordinate axis parallel with the bar, with x and y coordinates in the plane of any section, during twist there will be generated "warping" displacements "w" in the z direction, which are a function of x and y only.

If one or more of the following violations of the foregoing conditions exist, the torsion problem is a superposition of St. Venant Torsion and "warping" or "non-uniform" torsion.

(1) Cross-section is variable.

(2) Torsional moment varies.

(3) Longitudinal restraints are imposed at any location.

In structural design applications, apart from torque-driven shafts, torsion is almost always non-uniform and is usually further complicated by beam bending due to transverse loads. Non-uniform torsion combined with bending is also a problem in lateral-torsional buckling problems. Non-uniform aspects of the torsion problem are covered in many books and references and this report is concerned only with providing basic data for St. Venant torsion as applied to structural shapes.

The torsion constant for St. Venant torsion has the same relation to unit twist of a shaft as the moment of inertia has to the unit curvature of a beam bent under uniform moment. Thus, for uniform torsion,

$$M_z = J\, G\, \Theta \tag{1}$$

The derivation of the general St. Venant torsion theory is available in standard texts on the mathematical theory of elasticity and will not be presented in this report. The general solution is obtained from the following equation,

$$\frac{\partial^2 \psi}{\partial x^2} + \frac{\partial^2 \psi}{\partial y^2} = -2G\Theta \tag{2}$$

ψ is the "torsion stress-function" and the torsion constant is given by

$$J = \frac{2}{G\Theta} \iint \psi \, dx \, dy \tag{3}$$

at any location x, y, in the plane of the cross-section, the shear-stress components are

$$\tau_{zx} = \frac{\partial \psi}{\partial y}, \qquad \tau_{zy} = -\frac{\partial \psi}{\partial x} \tag{4}$$

and the magnitude of the resultant stress is therefore

$$\tau_{zr} = \sqrt{\tau_{zx}^2 + \tau_{zy}^2} = \sqrt{\left(\frac{\partial \psi}{\partial x}\right)^2 + \left(\frac{\partial \psi}{\partial y}\right)^2} \tag{5}$$

Prandtl[2] in 1903 noted that if a thin membrane (devoid of shear strength, such as a soap film) is stretched across a hole having the shape of a cross section, with a slight differential in pressure on the two sides of the membrane, the equation of the surface displacement

is identical in form with Equation (2), as follows:

$$\frac{\partial^2 \zeta}{\partial x^2} + \frac{\partial^2 \zeta}{\partial y^2} = \frac{-p}{T} \tag{6}$$

where

ζ = displacement of film in z direction.

p = pressure differential causing film to deflect.

T = tension force in the film per unit width (constant).

The analogy between Equations (2) and (6) illustrates the fact that the magnitude of the torsion stress function ψ may be thought of as a displacement, tracing out a continuous "stress-function" surface, and that the integral in Equation (3) is the volume under the surface. The slope of the stress-function surface represents the magnitude of the shear stress component in the x-y plane in a direction 90° to the direction for which the slope is evaluated. Contour lines, therefore, give the direction of maximum or resultant shear stress. The boundary of an open cross-section is equivalent to a contour line and on the boundary the value of ψ may be taken as zero. (It should be noted that the magnitude of maximum shear stress in general will vary along a contour line and will be inversely proportional to the spacing of the contour lines.)

In the case of circular sections, plane right cross-sections prior to twist remain plane after twist, and the shear stress is proportional to the distance from the central axis of the shaft. In this case the torsion constant "J" (Equations 1 and 3) is equal to the polar moment of inertia. The maximum shear stress at the boundary of the circular section is given by the simple expression

$$\tau_m = \frac{M_z r}{J} \tag{7}$$

The polar moment of inertia would be the torsion constant for non-circular sections, also, if the resultant shear stress were everywhere proportional in magnitude to the distance from the center of twist and directed at 90° to radial lines. The torsion constant of a non-circular section is always less than the polar moment of inertia - increasingly so as a section becomes less and less compact.

The present investigation is in part a sequel to earlier work whereby the membrane analogy was used to evaluate the torsion constant for the wide flange and I-beam section.[3,4] On the basis of this earlier work, the torsion constants of all rolled wide flange and I-beam shapes had been evaluated.[5]

The advent of the electronic digital computer has provided a means whereby an accurate re-evaluation of the torsion constant could be made, avoiding the experimental errors involved in soap film tests. Thus, for the wide flange and I-beam sections the present study provides results that approximately confirm but provide greater precision than was possible in the earlier experimental work. For the channel and angle sections this report provides information that has not been fully available heretofore.

The procedure for building up the formulas for the torsion constant of structural shapes follows the pattern suggested by Trayer and March[6] in their investigation of aircraft strut sections whereby the added torsional rigidity due to the juncture of two rectangular component parts was denoted as "αD^4". D is the diameter of the largest circle that can be inscribed at the juncture of the two component parts

and α is either determined experimentally by means of soap film tests or numerically as in the present studies by means of the difference equations.

THE RECTANGLE AND TRAPEZOIDAL SECTIONS

The rigorous solution of Equation (2) for the boundary conditions of rolled shapes such as the channel, WF beam, etc., is not practicable. The relatively few "exact" solutions that are available include some shapes of only academic interest, such as the ellipse and equilateral triangle. The solution for the rectangular shape, however, as developed by St. Venant[1] is of considerable engineering importance, not only of itself, but by virtue of the fact that the usual structural shape is made up of component parts that are either rectangular or trapezoidal. The width-thickness ratio of any one of these parts is usually four or more, for which proportions the torsion constant can be accurately expressed by a simple formula. The "torsion constant" of a structural shape can then be approximated by summing the values of J for the component rectangular parts and adding the juncture effect connection as herein evaluated.

The evaluation of St. Venant's solution for the rectangular cross-section may be expressed as follows:

$$J = \frac{bt^3}{3} - 2Vt^4 \tag{8}$$

in which t = the thickness and b = the breadth of a rectangular section, and

$$\tau_m = \frac{M_z \gamma t}{J} \tag{9}$$

where V and γ are factors depending upon the ratio $\frac{b}{t}$ and are given by the following table.

TABLE 1

Ratio $\frac{b}{t}$	2V	γ
1.00	0.1928	0.6753
1.10	0.1973	0.7198
1.20	0.2006	0.7578
1.30	0.2031	0.7935
1.40	0.2050	0.8222
1.50	0.2064	0.8476
1.60	0.2074	0.8695
1.80	0.2086	0.9044
2.00	0.2093	0.9300
2.50	0.2099	0.9681
3.00	0.2101	0.9855
4.00	0.2101	0.9970
∞	0.2101	1.0000

The formula for the trapezoidal section, (Figure 1) as developed in Reference 4, can be written:

$$J = (b/12)(t_1^2+t_2^2)(t_1+t_2) - V_L t_2^4 - V_S t_1^4 \qquad (10)$$

V_L and V_S are the end constants V, for the thick end and the thin end, respectively, of the trapezoid.

$$V_L = 0.10504 - 0.10000\ S + 0.08480\ S^2 - 0.06746\ S^3 + 0.05153\ S^4 \qquad (11)$$

and,

$$V_S = 0.10504 + 0.10000\ S + 0.08480\ S^2 + 0.06746\ S^3 + 0.05153\ S^4 \qquad (12)$$

in which S = the total slope of the section or tangent of the slope angle. For certain particular values V_L and V_S are calculated in Table 2.

TABLE 2

STANDARD SLOPES

	V_L	V_S
1/6	0.09045	0.12441
1/20	0.10026	0.11026
1/50	0.10307	0.10707
1/∞	0.10504	0.10504

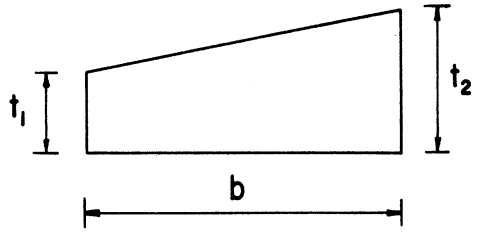

Figure 1

SOLUTION OF THE TORSION PROBLEM BY USE OF DIFFERENCE EQUATIONS

To provide solutions for complex boundary conditions not readily evaluated by analytical procedures, Equation (2) may be replaced by a "difference equation" and the solution obtained for any cross-section to any desired degree of approximation dictated by need and available computation time. For manual or desk calculator use, "relaxation" procedures of solution were initiated by Christopherson and Southwell.(7) Shaw(8) has applied these procedures with special emphasis to the torsion problem and has extended the application to include non-linear stress-strain relationships and closed sections. The foregoing references should be consulted for a more complete discussion of difference equations for the torsion problem and for a review of relaxation methods.

In one form of the difference equation procedure the value of the torsion stress-function, ψ, is determined approximately at the points of intersection (nodal points) of a network of squares formed by equally spaced lines (Figure 2), parallel to the x and y axis in the plane of the cross-section. For any point "0" (Figure 2), Equation (2) may be written in terms of neighboring nodal points as follows:

$$(\psi_1 + \psi_2 + \psi_3 + \psi_4 - 4\,\psi_o) = -\,2\,H^2\,G\,\Theta \qquad (13)$$

in which H is the mesh size. ψ may be replaced by ϕ, where ϕ is a dimensionless quantity, taken so that

$$\psi = \frac{2H^2G\Theta}{R_o}\,\phi \qquad (14)$$

R_o = any convenient constant introduced for the purpose of making the ϕ's large numbers for ease of numerical manipulation. Equation (13) with this substitution becomes

$$(\phi_1 + \phi_2 + \phi_3 + \phi_4 - 4\phi_0) = -R_o \qquad (15)$$

Points on the boundary will not usually coincide with the points of the square net. For this case, a special finite difference equation may be derived.[11] Referring to Figure 3a, the nondimensional finite difference equation at point "0" for Equation (2) will be:

$$\frac{\phi_1}{M} + \frac{\phi_2}{N} + \frac{\phi_3}{R} + \frac{\phi_4}{K} - \phi_0 \left(\frac{1}{M} + \frac{1}{N} + \frac{1}{R} + \frac{1}{K}\right) = -R_o \left(\frac{M+N+R+K}{4}\right) \qquad (16)$$

when $M = K = 1$, and $\phi_2 = \phi_3 = 0$ (Figure 3b), Equation (16) reduces to

$$\phi_1 + \phi_4 - \phi_0 \left(2 + \frac{1}{R} + \frac{1}{N}\right) = -R_o \left(\frac{2 + N + R}{4}\right) \qquad (17)$$

when $M = K = N = R = 1$, Equation (16) reduces to Equation (15) as derived for a square net.

Special "block" relaxation techniques developed to aid convergence in manual solution are not particularly helpful in computer analysis. The computer is programmed to make a simple repetitive scanning of the node points with ϕ at each point "0" calculated by Equation (15), rewritten as follows:

$$\phi_0 = \frac{1}{4}(\phi_1 + \phi_2 + \phi_3 + \phi_4 + R_o) \qquad (18)$$

It is helpful if a guess can be made for initial values of ϕ. In the present investigation there was a sequential variation of dimensional parameters in the analysis of structural shape intersection regions. In the first analysis of a given set of parameters, initial ϕ's were set

at zero, but for succeeding analyses, for which minor variations were made in a particular dimensional parameter, the initially assumed values were those of the previous computer run. Thus convergence subsequent to the first run of a sequence was rapid.

In order to calculate the volume under the stress function surface, as approximated by nodal values of ϕ, the computer met conditions illustrated in Figure 4.

Whenever the volume could conveniently be calculated under a 2H by 2H square, as in regions A of Figure 4a, the double application of Simpson's Rule gave a good approximation. Referring to Figure 4b,

$$\iint_A \phi dxdy = \frac{(2H)^2}{36} \{(\phi_5 + \phi_6 + \phi_7 + \phi_8) + 4(\phi_1 + \phi_2 + \phi_3 + \phi_4) + 16\,\phi_0\} \qquad (19)$$

When a single whole square was involved, as in regions B of Figure 4a, the volume was computed by the following equation, as used in the same situation by Shaw,[8] which incorporates a correction for the usual convexity of the stress-function surface. (The numbers are for one quadrant of the 2H by 2H surface in Figure 4b).

$$\iint_B \phi dxdy \simeq \left(\frac{\phi_5 + \phi_1 + \phi_2 + \phi_0}{4} + \frac{R_0}{24}\right) H^2 \qquad (20)$$

For the various triangular areas along the curved boundary of Figure 4, as represented by Figure 4c, the volume was calculated by

$$V = \frac{NRH^2}{6} (\phi_0 + \phi_2 + \phi_3) \qquad (21)$$

The results of a typical computer calculation are shown in Figure 5 for the intersection region of a web and sloping flange such

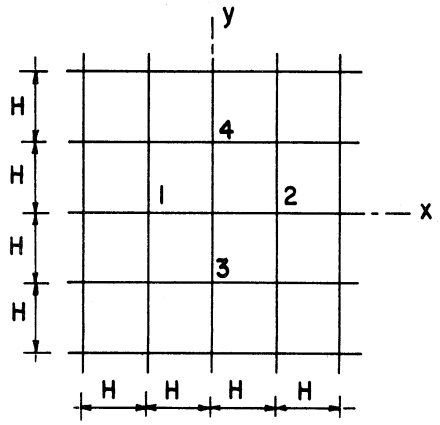

Figure 2

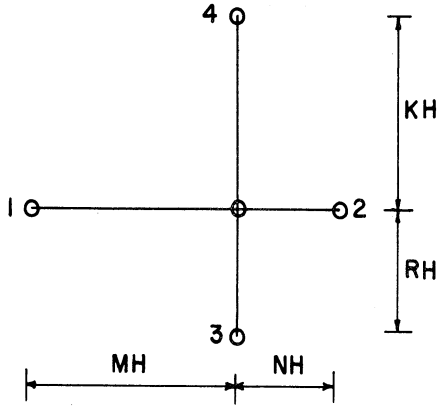

Figure 3 (a)

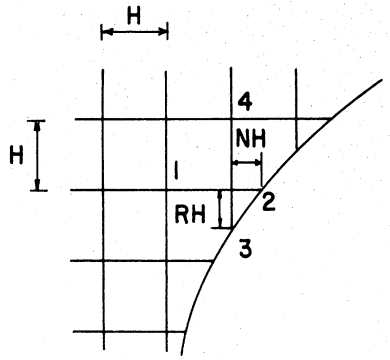

Figure 3 (b)

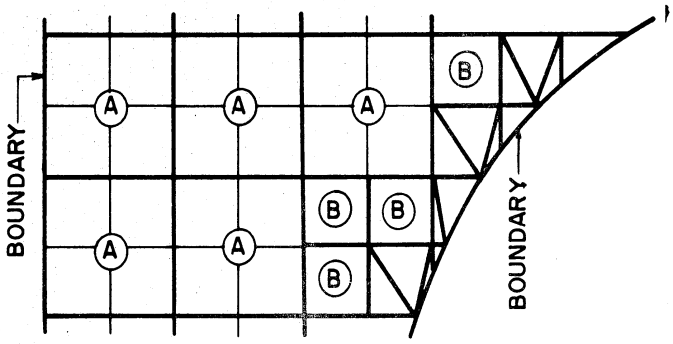

Figure 4 (a)

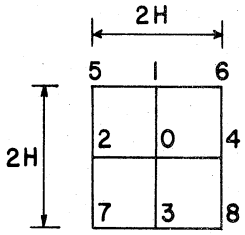

Figure 4 (b)

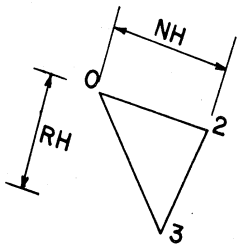

Figure 4 (c)

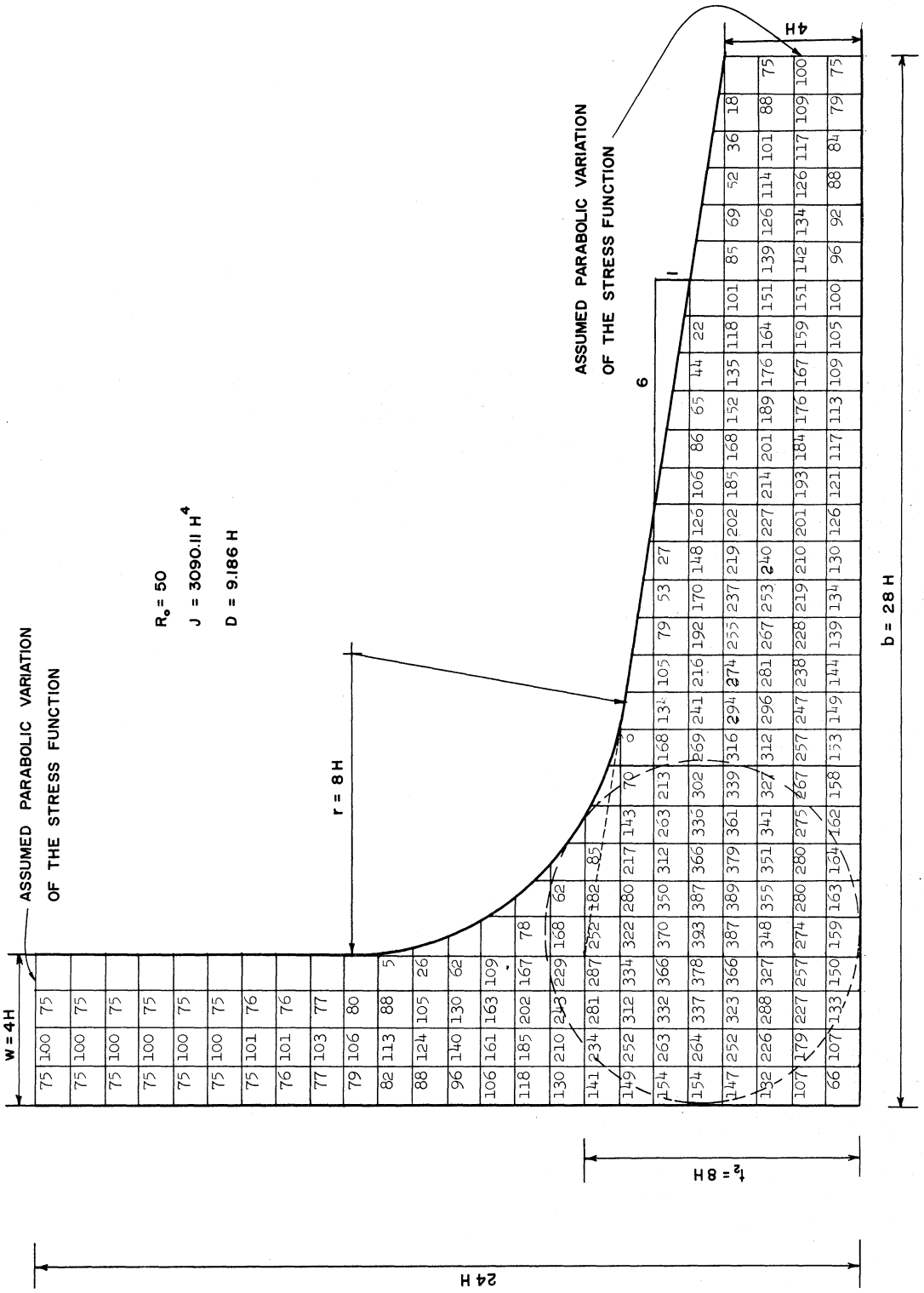

Figure 5. Typical Example of Computer Output Giving Stress Function Ordinates Rounded Off as Shown.

as occurs at a corner of a standard channel. At each extremity, the boundary value of ϕ has been assumed parabolic, as for the interior of a narrow rectangular or trapezoidal section. The figure written in each square represents the computer calculation for ϕ at the upper right hand corner rounded off without digits to the right of the decimal point. The values actually used by the computer to calculate J were accurate to several additional significant figures.

THE TORSION CONSTANT OF STRUCTURAL SECTIONS

The essential or missing element required for the accurate calculation of the torsion constant of a structural shape is illustrated by Figure 6 for the four cases herein considered. On the left side, labeled (a), are the arbitrary assignments of rectangular or trapezoidal areas and end conditions which account for the bulk of the torsion constant contributed by these regions. When a rectangular or trapezoidal element is bounded at either end by a dashed line (Figure 6), the variation in stress-function along the dashed line has been assumed parabolic and equivalent to the variation across the thickness in the interior of a rectangle of indefinite extent, rather than zero as it would be at the end of a rectangular cross section. The length of the extremities were several times the thickness of the part beyond the fillet tangent point, as illustrated in Figure 5, thus assuring complete evaluation of the juncture effect to any reasonable degree of needed accuracy.

At the juncture, various choices could be made as to end conditions or arrangement of trapezoidal and rectangular components - it is important only that the same conditions be reflected in the way the torsion constant is synthesized in the formulas to be presented later for the various structural shapes.

The total correction represents the difference between the computer calculated constant for the tee or angle in Figure 6b and the summation of constants for the rectangles or trapezoids in Figure 6a by Equations (8) or (10), with appropriate deletion of the negative

CORRECTION

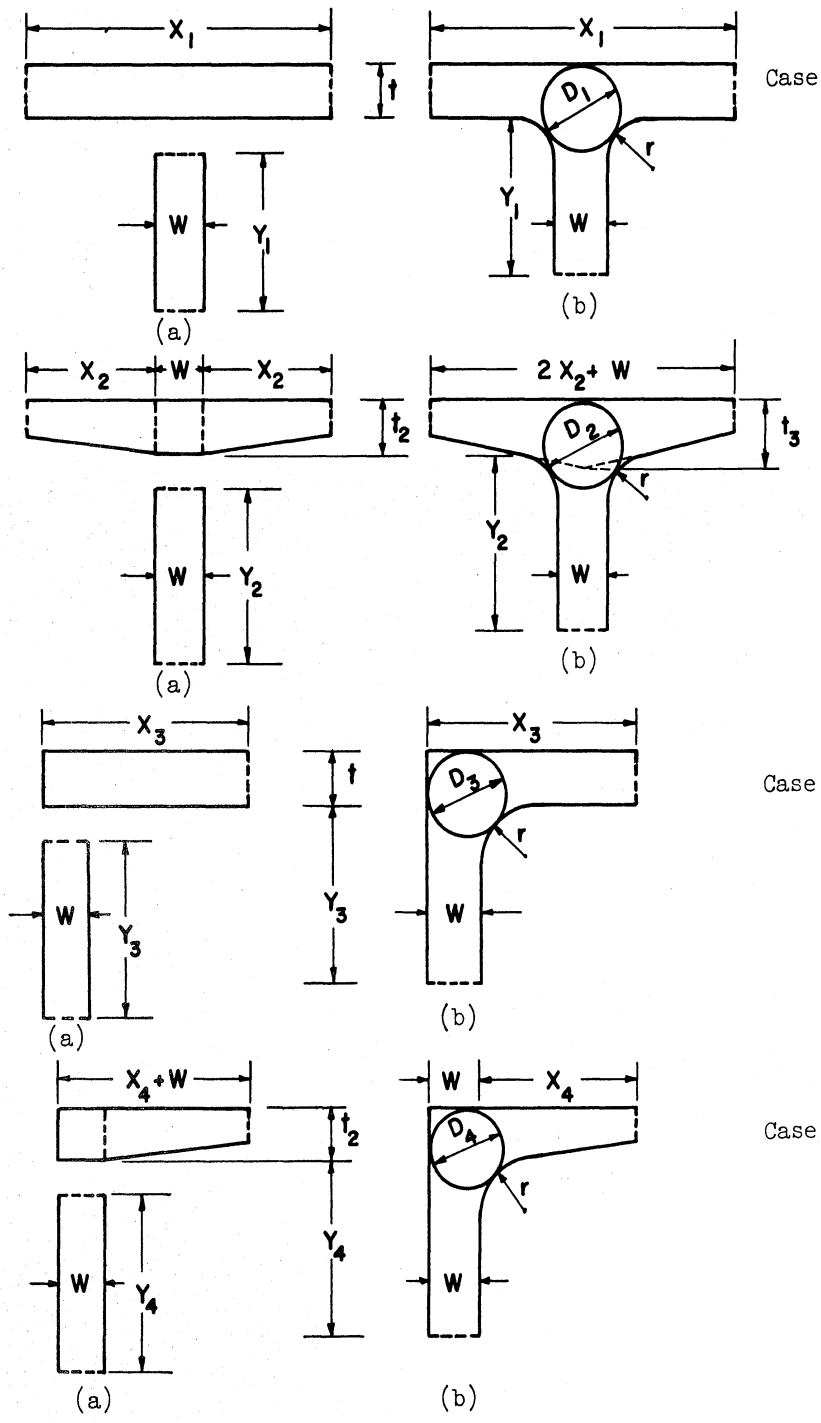

Case 1. Parallel Flange Tee
$\alpha_1 D_1^4$

Case 2. I-Section Tee
$\alpha_2 D_2^4$

Case 3. Angle Section
$\alpha_3 D_3^4$

Case 4. Angle Section of Standard Channel
$\alpha_4 D_4^4$

Figure 6. Basis for Tee or Angle Juncture Corrections for Torsion Constant of WF, I, Tee, Channel, Zee, and Angle Shapes.

terms for ends of cross-sections which have dashed lines. The correction coefficients α are made dimensionless by the introduction of D^4 where D is the diameter of the largest circle that can be inscribed at the juncture point. Thus,

$$\alpha = \frac{1}{D^4} \left\{ \begin{array}{l} (\text{Computed J of tee or angle}) \\ - \\ (\text{J of arbitrarily chosen segments shown in Figure 6}) \end{array} \right\} \quad (22)$$

Corresponding to the four cases of Figure 6, formulas for "D" are given in Table 3.

TABLE 3

EQUATIONS FOR D IN FIGURE 7

(S is the flange slope, i.e., tangent of the slope angle)

Case 1 Parallel Flange Tee Segment

$$D_1 = \frac{(t+r)^2 + w(r + \frac{w}{4})}{2r + t} \quad (23)$$

Case 2 I-Section Tee Segment

$$D_2 = \frac{(F+t_3)^2 + w(r + \frac{w}{4})}{F + r + t_3} \quad (24)$$

where

$$F = r S \left(\sqrt{\frac{1}{S^2} + 1} - 1 - \frac{w}{2r} \right)$$

Case 3 Angle Segment

$$D_3 = 2 \left\{ (3r + w + t) - \sqrt{2(2r + w)(2r + t)} \right\} \quad (25)$$

Case 4 Angle Segment of Standard Channel

$$D_4 = 2 \left\{ (3r + w + H) - \sqrt{2(2r + w)(2r + H)} \right\} \quad (26)$$

where

$$H = t_2 - r (S + 1 - \sqrt{1 + S^2})$$

Computer analyses were made for approximately thirty different proportions for each of the four cases shown in Figure 6. For each case there was a systematic variation between zero and one of the (fillet radius)/(flange thickness) ratio (r/t) or (r/t_2) and the (web)/(flange) thickness ratio, (w/t) or (w/t_2). The resulting values of α for the four cases are plotted in Figures 7, 8, 9, and 10, respectively, by solid lines. For structural sections having flanges with slopes other than 1 in 6, a good approximation for α may be made by interpolating linearly between $S = 0$ and $S = 0.1667$.

Also shown on Figures 7, 8, 9, and 10 are dashed lines plotted from the following empirical formulas and applicable in the range for which they are shown as a reasonable approximation for α.

$$\alpha_1 = -.0420 + .2204\,\frac{w}{t} + .1355\,\frac{r}{t} - .0865\,\frac{wr}{t^2} - .0725\left(\frac{w}{t}\right)^2 \qquad (27)$$

$$\alpha_2 = -.0836 + .2536\,\frac{w}{t_2} + .1268\,\frac{r}{t_2} - .0806\,\frac{wr}{t_2^2} - .0858\left(\frac{w}{t_2}\right)^2 \qquad (28)$$

$$\alpha_3 = -.0908 + .2621\,\frac{w}{t} + .1231\,\frac{r}{t} - .0752\,\frac{wr}{t^2} - .0945\left(\frac{w}{t}\right)^2 \qquad (29)$$

$$\alpha_4 = -.1325 + .3015\,\frac{w}{t_2} + .1400\,\frac{r}{t_2} - .1070\,\frac{wr}{t_2^2} - .0956\left(\frac{w}{t_2}\right)^2 \qquad (30)$$

In each of the foregoing cases (Equations 27 - 30) the empirical formula gives a good approximation for α in the range

$$0.2 < (r/t) < 1.0$$

$$0.5 < (w/t) < 1.0$$

Generally, the corrective term αD^4 is positive, but for Case 2 (the sloping flange tee intersection) it may become negative when w/t_2 is less than 0.4 for varying amounts of r/t_2 ranging from

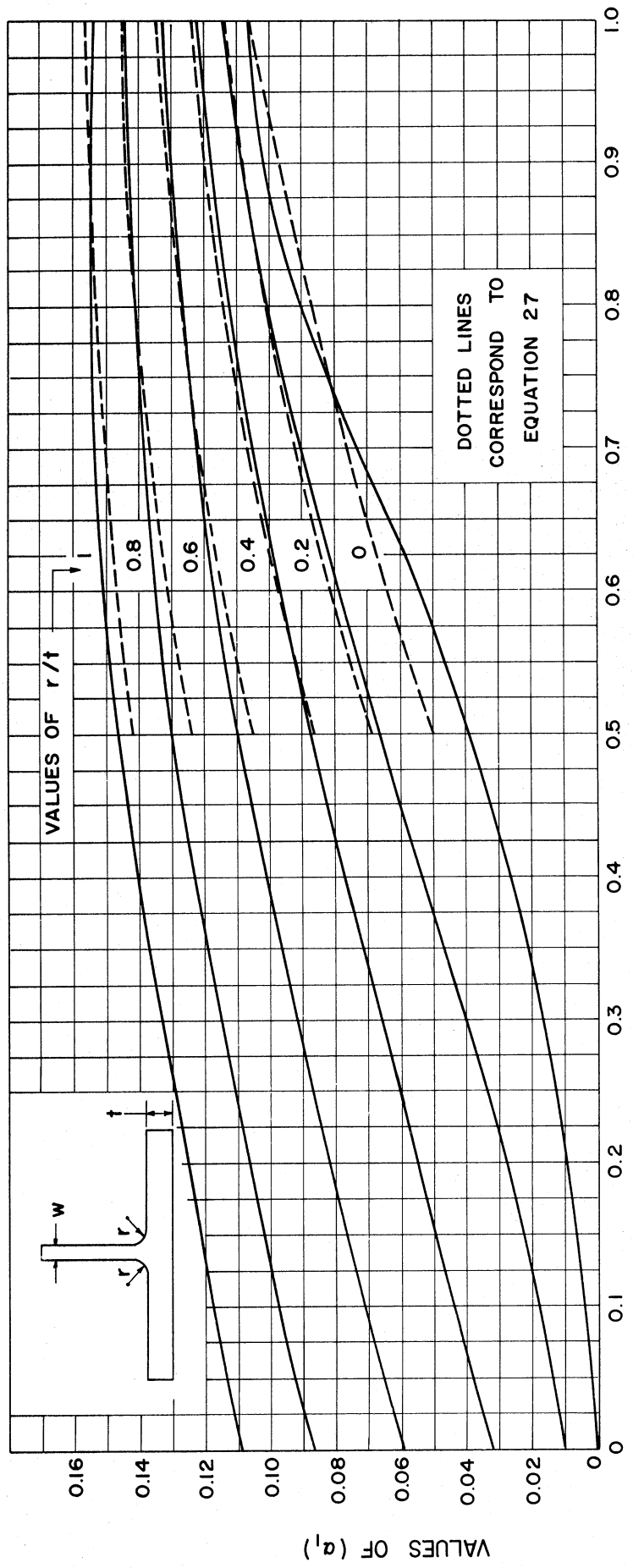

Figure 7. Values of (α_1) for Parallel Flange Tee Shapes.

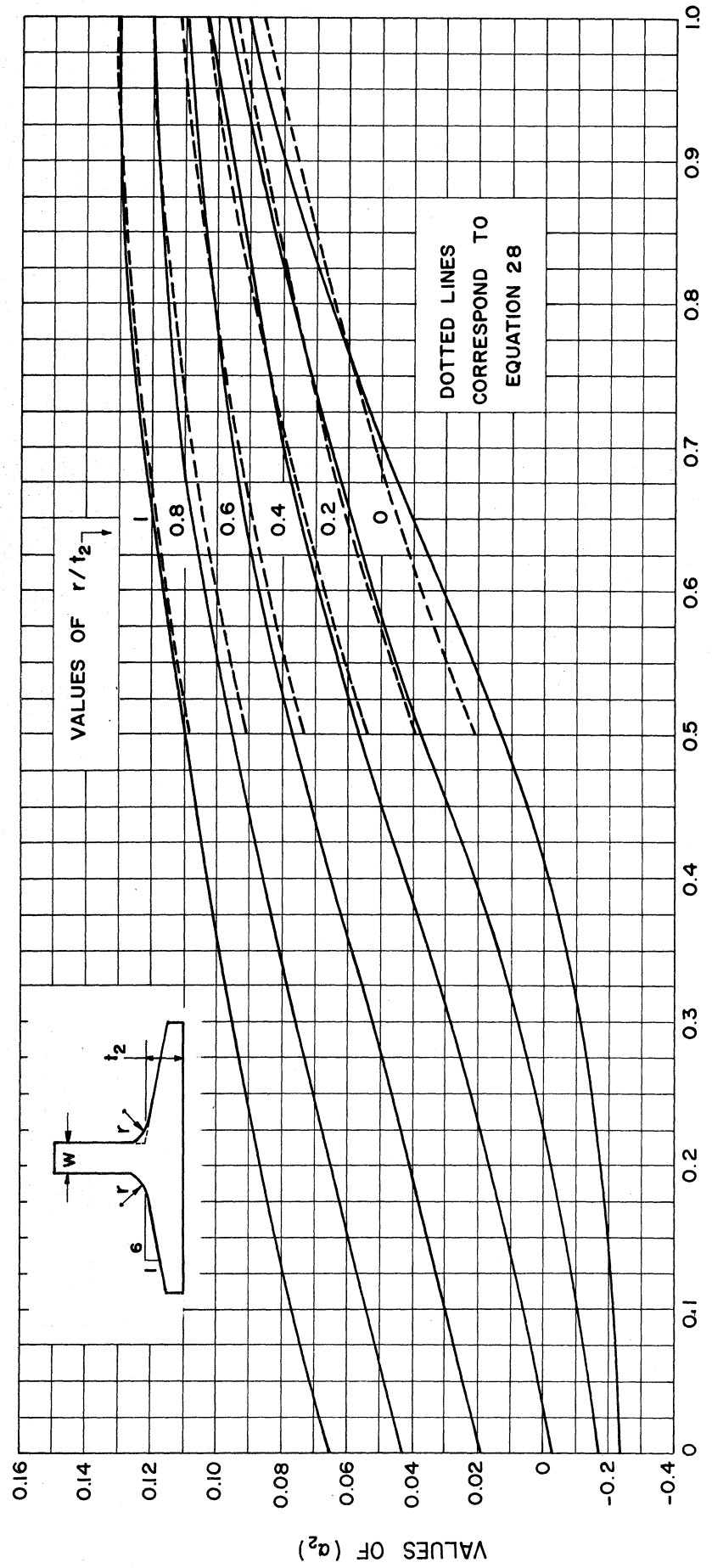

Figure 8. Values of (α_2) for I Section Tee Shapes Flange Slope 1/6.

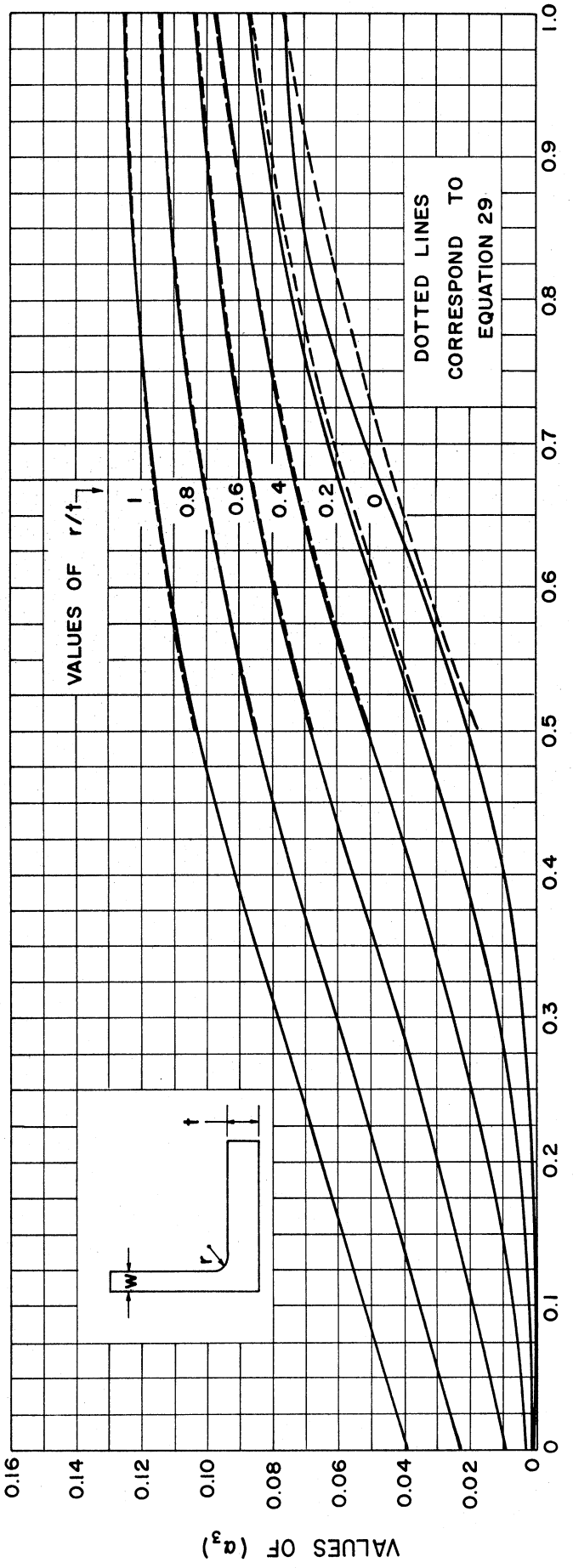

Figure 9. Values of (α_3) for Parallel Flange Angle Section.

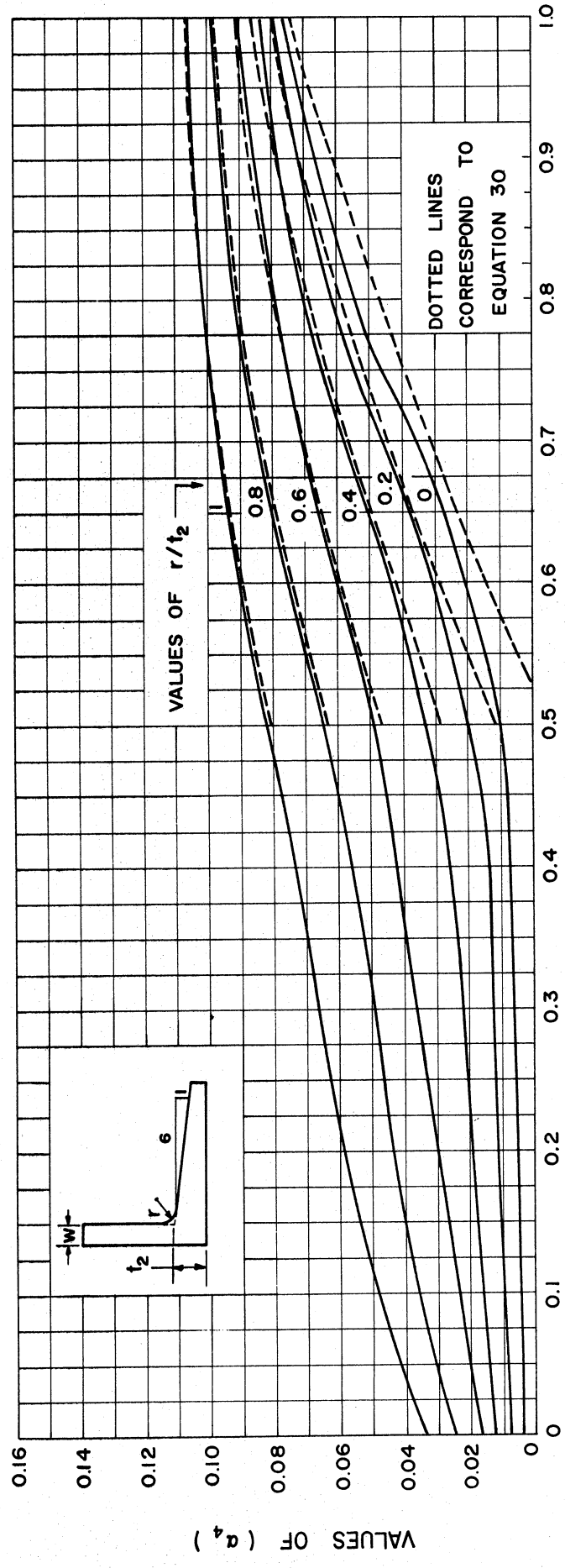

Figure 10. Values of (α_4) for Angle Section of Standard Channels Flange Slope 1/6.

0 up to about 0.4. This can be explained by means of Figure 11, which is Case 2 for both w/t_2 and r/t_2 equal to zero. In this case J of the trapezoidal segments of Case 2(a) (Figure 6) would be calculated by Equation (10) without any end loss (V_S or V_L) terms. Obviously, the stress-function surface must have a zero slope in the long direction at the central discontinuity, as shown for actual computed $\not\subset$ values in Figure 11. The assumption of parabolic variation across the thickness at the $\not\subset$ (adjoining large ends of the two trapezoidal segments) gives a greater stress function value and an incorrect discontinuity of surface. In Figure 11 the maximum ordinates of a parabolic variation of the stress-function, on which Equation (10) is based, is plotted (without end loss) along the longitudinal sloping centerline of adjoining trapezoidal sections of dimensions $t_2 = 8$ H, $S = 1/6$, and $b = 24$ H. In the same figure the computed centerline stress function (ϕ) is also plotted. The value of J obtained from the computer is 1871.6 H^4 as compared with 1920 H^4 by Equation (10) (without end loss). Twice the area of the hatched area in Figure 11 times two thirds of the width of the trapezoid at its center of gravity is found to be 45.0 H^4, which very nearly accounts for the foregoing difference.

For the angle section with legs of equal thickness, the value of α can be interpolated at the extreme right boundary of Figure 9. Figure 12 gives a more accurate evaluation of α for angles with legs of equal thickness, particularly when the fillet radius is large. In this particular case, the values of α were computed for fillet radii up to six times the flange thickness. This is far greater than the range of rolled structural angles but was computed to afford a comparison

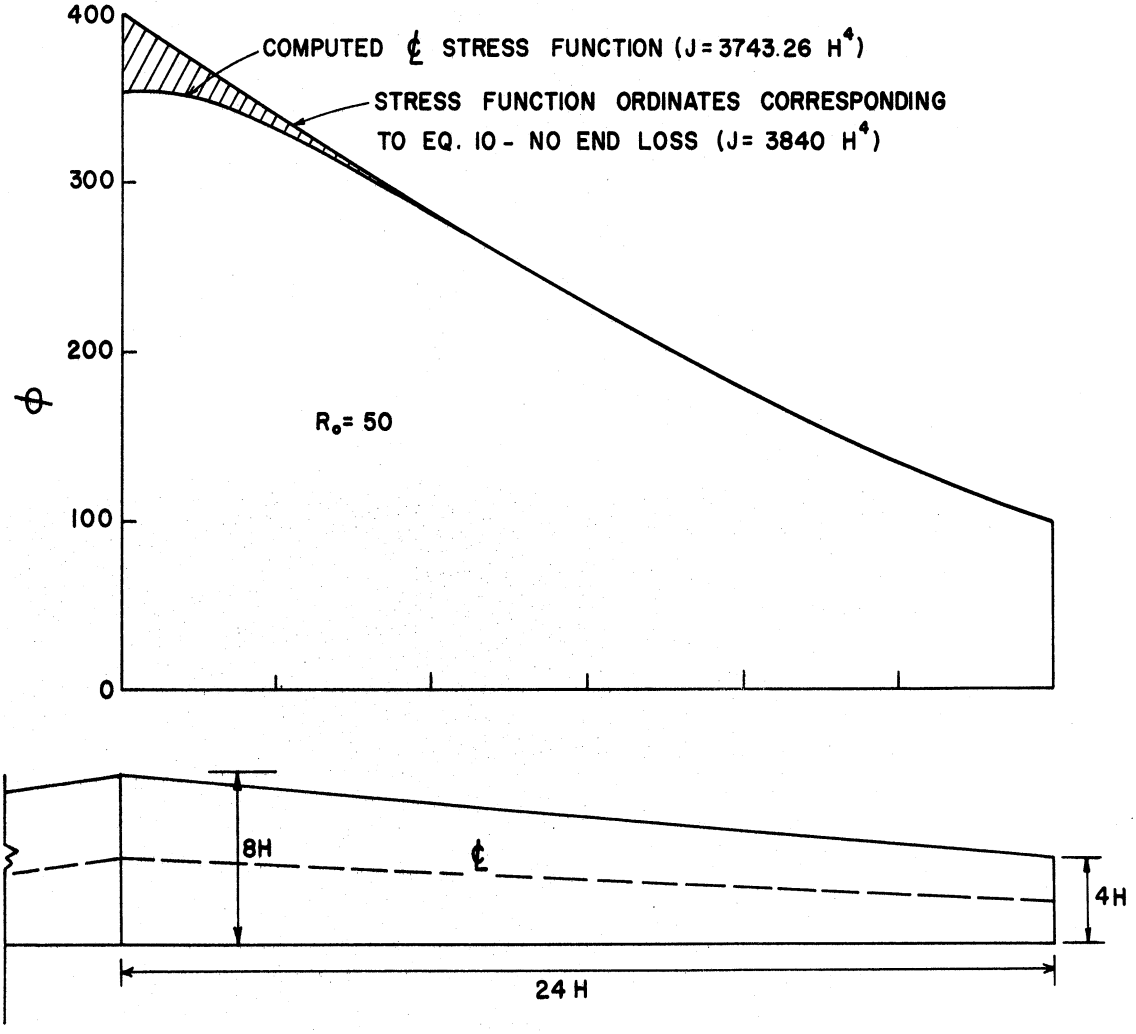
400
300
200
100
0
θ
COMPUTED ℄ STRESS FUNCTION (J = 3743.26 H⁴)
STRESS FUNCTION ORDINATES CORRESPONDING
TO EQ. 10 - NO END LOSS (J = 3840 H⁴)
R₀ = 50
8H
℄
4H
24 H

Figure 11.

with the work of other investigators in these ranges. Figure 12 also plots the empirical formulas suggested by Trayer and March,[6] which were based on their tests. In addition, the results of both experimental tests and numerical analyses by the relaxation technique, as carried out by Cullimore and Pugsley,[9] are plotted together with the two straight line formulas that they propose. The present computer analyses plot midway within the scatterband of results of Cullimore and Pugsley for small fillet radii and agree very well with their results as the radius becomes large. Also shown on Figure 12 is the plot of a proposed empirical formula that agrees well with the computer analyses made for this report.

$$\alpha = 0.0728 + 0.0571 \left(\frac{r}{t}\right) - 0.0049 \left(\frac{r}{t}\right)^2 \qquad (31)$$

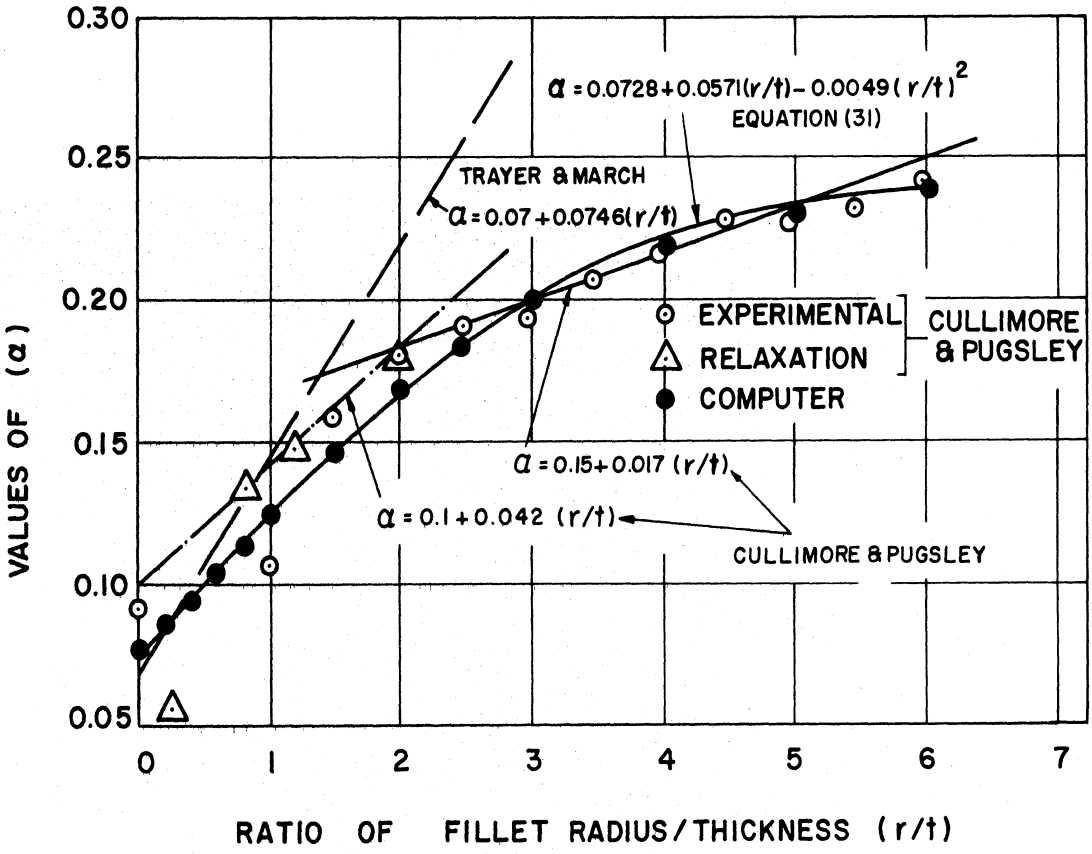

Figure 12. Angle Correction Coefficient (α) for Angle Intersection with Equal Thickness Legs.

MAXIMUM SHEAR STRESS DUE TO TORSION

A number of approximate formulas have been developed to give an indication of the stress concentration factor in a fillet for a structural member in uniform torsion. For the rectangular cross-section of large b/t ratio, the maximum shear stress at the center of the wide face is

$$\tau_m = \frac{M_z t}{J} \tag{32}$$

When the breadth-thickness ratio of a rectangle is less than 4 the maximum torsional stress is less than as given by Equation (32), dropping down to 0.6753 times this value for the square section. St. Venant[1] gives a complete tabulation. (See Table 1.)

For an angle section with equal legs, it is obvious because of symmetry about a line from the corner at 45 degrees to the angle face that, for angles having large width-thickness ratios, the maximum stress due to torsion is at the intersection of the 45 degrees line from the corner and the inside angle fillet. As the fillet radius becomes large, the stress concentration effect must decrease but the actual stress due to torsion increases because of the greater thickness of material in this juncture region. If the total stress increase is given as a percentage increase above that in the body of the angle away from the fillet, as given by Equation (32), results of various investigators are plotted in Figure 13.

The curves in Figure 13 that rise at the right side of the figure reflect the increasing effect of thickness that overbalances the

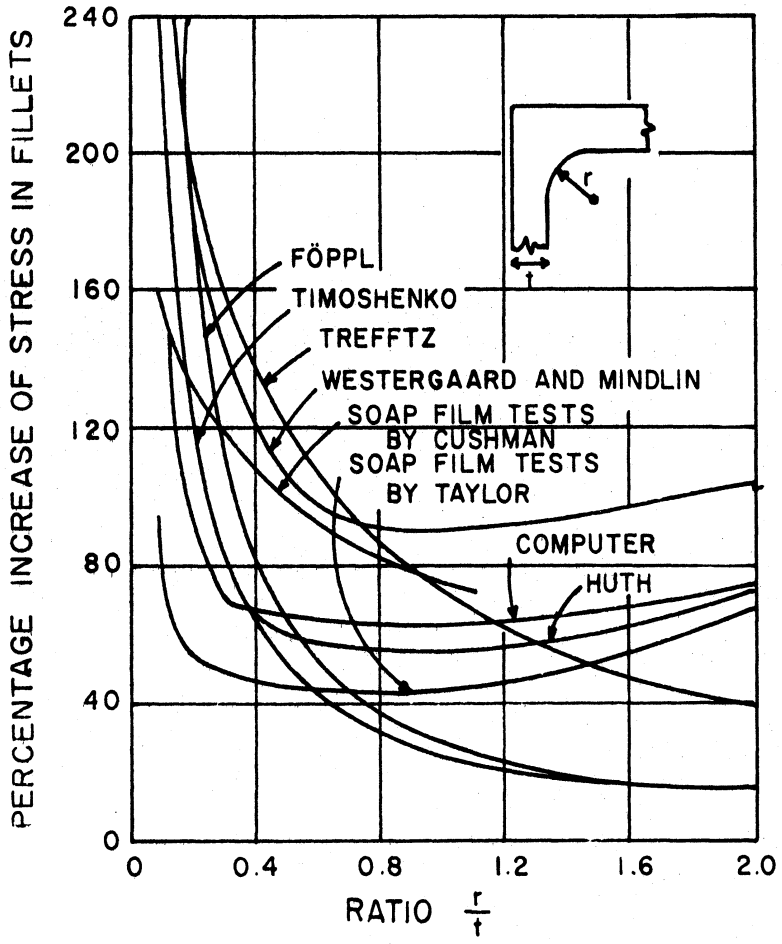

Figure 13. Formulas for Stress Increase in Fillets Due to Torsion.

diminishing effect of stress concentration as the fillet radius increases. This is true, of course, for the curve labeled "computer solution" which is based on the results of the present investigation. These results agree very well with those of Huth[10] who wrote a rather complete discussion of the earlier results shown on Figure 13. Huth suggests that "the stress concentration in angle sections with generous fillets may be lowered considerably by rounding off the outside corner in such a way as to keep the thickness of the section everywhere approximately constant." Such a suggestion overlooks the fact that more is gained due to increased torsion constant as this juncture increases in thickness than is lost by the so-called "stress concentration factor for generous fillets" which is not a stress concentration but merely an indication of the effect of increased thickness on shear stress. Thus, for very "generous fillets," the actual stress for a given torsional moment will always continue to decrease as the fillet radius increases, all other dimensions remaining the same. It may also be noted that the curve resulting from Timoshenko's approximation solution[11] does diminish as the fillet radius increases and thus is probably a very good approximation of the actual stress increase since it agrees very well in the lower ranges with that obtained in the present investigation as well as the similar results obtained by Huth. It is believed that the results of the present investigation may be considered to be quite accurate since the mesh size used was relatively much smaller than would be feasible for desk calculator operation using relaxation techniques.

For the T juncture section there is a maximum stress on the outer face of the flange at the intersection with the midplane of the web.

This is an important stress location since at this point shear stress is combined with maximum shear stress due to flange bending that occurs in problems of nonuniform torsion. Here, also, the stress reflects only the increased thickness of the juncture since there can be no stress concentration effect on the flat surface. Figures 14 and 15 give values of δ to be used in the following Equation (33) as a measure of maximum shear stress as a function both of fillet radius and webbed flange thickness.

$$\tau_{max} = \frac{\delta M_z t}{J} \tag{33}$$

For the I beam with flange slope of 1/6, "t_2" (see Figure 6) is to be used in Equation (33) in the place of "t".

Stresses will be greater than as given by Equation (33) in the fillets on the inner side of the flange but the location can no longer be predetermined as in the case of the angle with equal thickness legs. A similar observation could be made regarding the stresses on either face of the angle channel type segment or the angle with different thickness legs. The results of the present program are available to permit a more complete study of these stresses but these will be reported upon in a later paper.

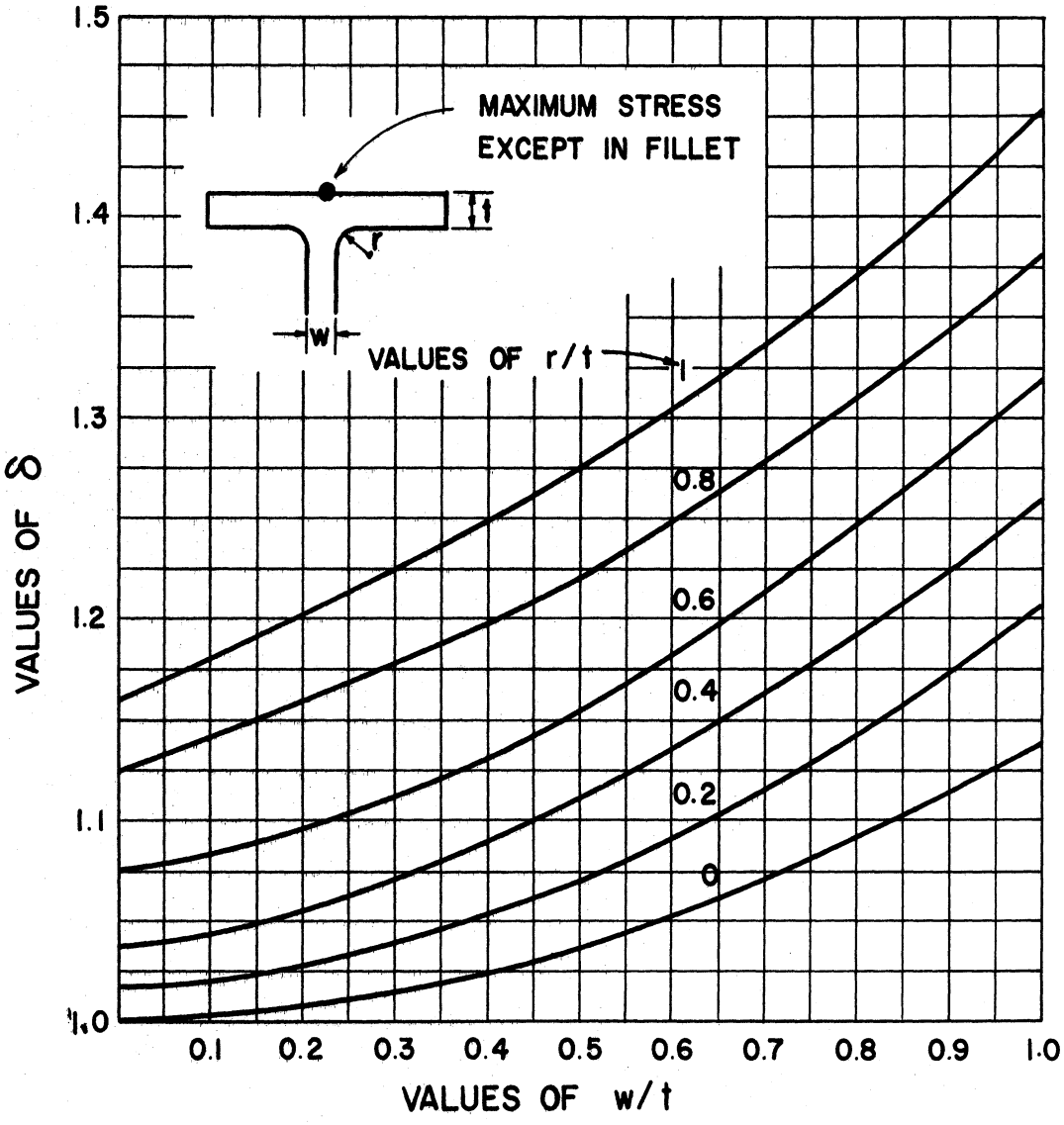

Figure 14. Coefficient of Stress Increase for Tee or WF Section With Parallel Sided Flange.

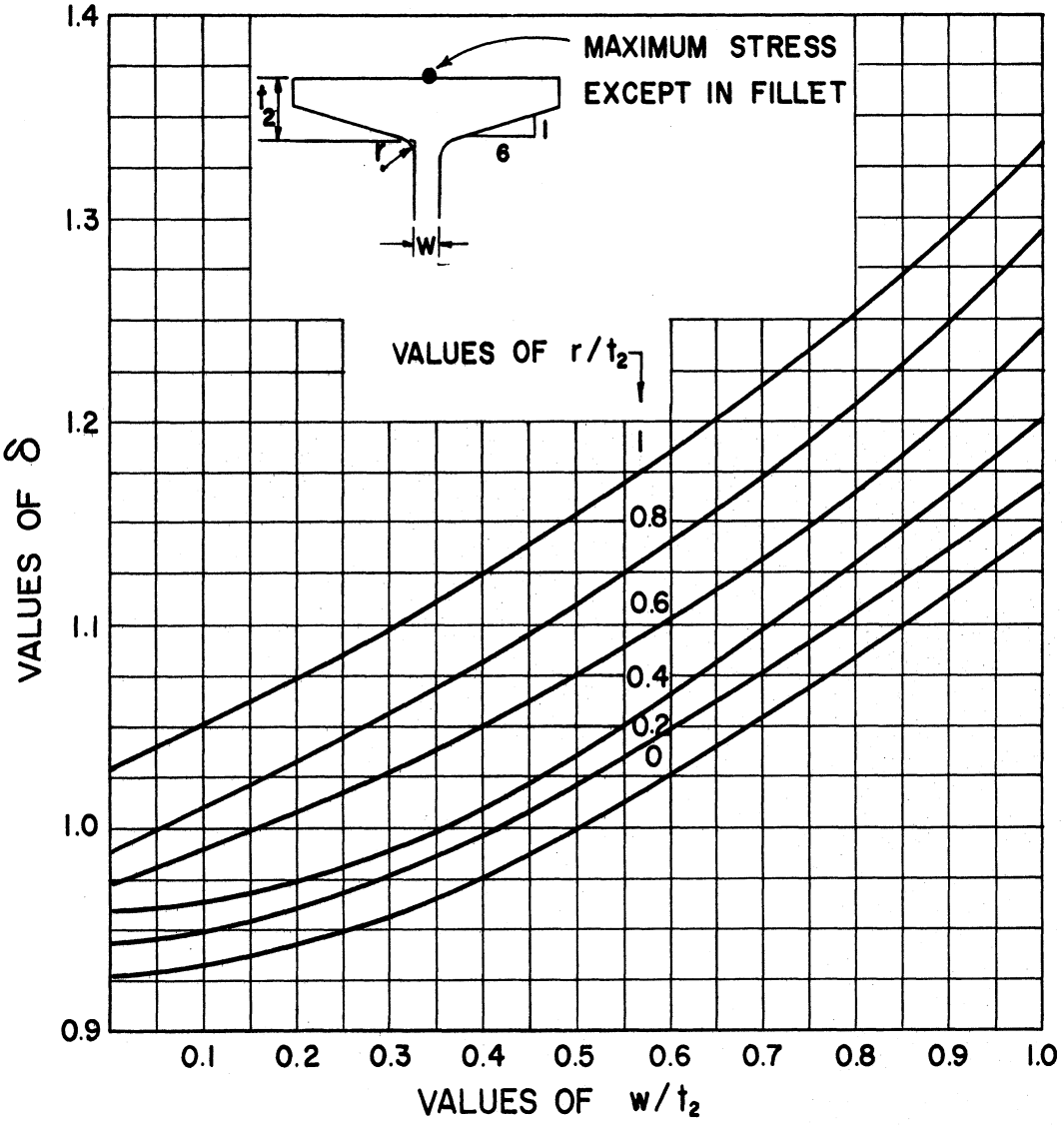

Figure 15. Coefficient for Maximum Stress Determination in Outside Face of Tee or I-Section with 1 - 6 Flange Slope.

TORSION CONSTANTS FOR STRUCTURAL SHAPES

The value of "α" applicable to a particular structural shape is determined from Figures 7, 8, 9, or 10, or, less approximately from Equations (27), (28), (29), or (30). The correction for the juncture effect then can be computed and added to the known contributions of the various component parts to the torsion constant. For the special case of the angle with legs of equal thickness, α may be obtained from Figure 12 or by Equation (31).

After α is determined, the torsion constant J for any one of the nine different structural shapes shown in Figure 16 is readily calculated by the appropriate equation (Equations 34 through 41).

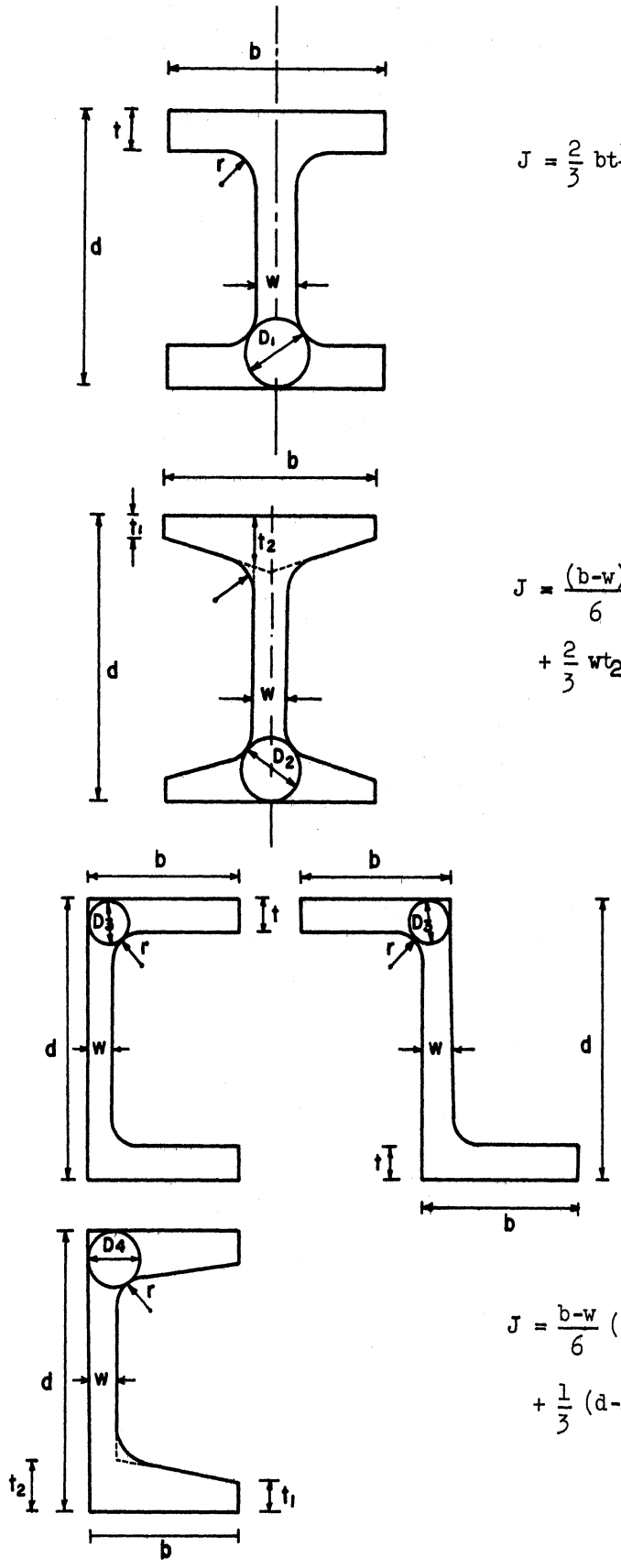

$$J = \frac{2}{3} bt^3 + \frac{1}{3} (d-2t)\, w^3 + 2\alpha_1 D_1{}^4 - .420\, t^4 \qquad (34)$$

$$J = \frac{(b-w)}{6} (t_1 + t_2)(t_1{}^2 + t_2{}^2) + \frac{2}{3} wt_2{}^3 + \frac{1}{3} (d-2t_2)\, w^3 + 2\alpha_2 D_2{}^4 - 4\, V_S t_1{}^4 \qquad (35)$$

$$J = \frac{2}{3} bt^3 + \frac{1}{3} (d-2t)\, w^3 + 2\alpha_3 D_3{}^4 - .420\, t^4 \qquad (36)$$

$$J = \frac{b-w}{6} (t_1 + t_2)(t_1{}^2 + t_2{}^2) + \frac{2}{3} wt_2{}^3 + \frac{1}{3} (d-2t_2)\, w^3 + 2\alpha_4 D_4{}^4 - 2V_S t_1{}^4 - .210\, t_2{}^4 \qquad (3$$

Figure 16. Summary of Formulas for Torsion Constants for Structural Shapes.

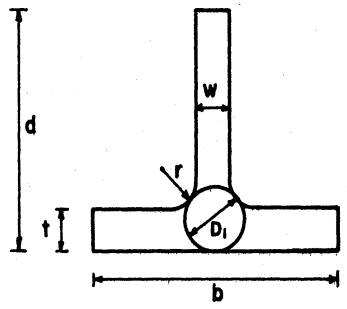

$$J = \frac{1}{3} bt^3 + \frac{(d-t)}{3} w^3 + \alpha_1 D_1^4 - .210\ t^4 - .105\ w^4 \qquad (38)$$

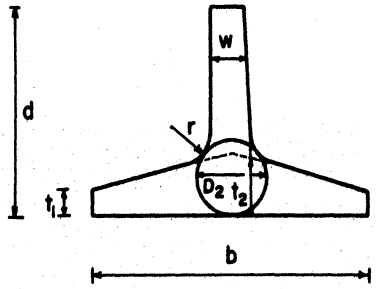

$$J = \frac{b-w}{12} (t_1 + t_2)(t_1^2 + t_2^2) + \frac{1}{3} wt_2^3 + \frac{1}{3} (d-t_2)\ w^3 + \alpha_2 D_2^4 - 2V_S t_1^4 - .105\ w^4 \qquad (39)$$

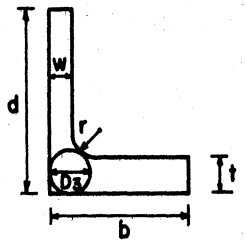

$$J = \frac{1}{3} bt^3 + \frac{(d-t)}{3} w^3 + \alpha_3 D_3^4 - .210\ t^4 - .105\ w^4 \qquad (40)$$

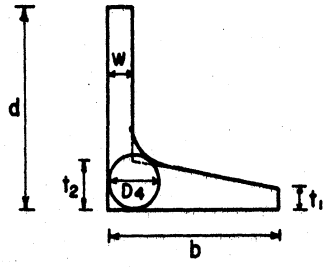

$$J = \frac{b-w}{12} (t_1 + t_2)(t_1^2 + t_2^2) + \frac{1}{3} w\ t_2^3 + \frac{1}{3} (d-t_2)\ w^3 + \alpha_4 D_4^4 - V_S t_1^4 - .105\ t_2^4 - .105\ w^4 \qquad (41)$$

Figure 16. (Continued)

ACCURACY AND COMPARISON WITH PRIOR TEST RESULTS

The accuracy of the computer program results were tested by comparison with the known torsion constant for the rectangular section. Using a section of thickness 8 H and breadth 48 H, the computer analysis gave a value of $J = 7320.58\ H^4$ while the St. Venant solution gave a value of $J = 7331.42\ H^4$, a difference of about 0.15 per cent.

The effect of mesh size "H" was also studied. For the channel segment, as shown in Figure 5, with $r/t_2 = 1$ and $w/t_2 = 0.5$, as shown, α for the juncture correction factor was found to be 0.080927. For a mesh size 2/3 of that shown on Figure 5, an α of 0.081334 was obtained and an H^2 extrapolation of the two results yields a value of 0.08166, thus indicating a probable error in the values of α of less than 1 per cent for this particular case. Since the juncture correction factor for the channel is usually less than 10 per cent, this means that the overall error in the torsion constant would usually be less than 0.10 per cent and the final values of the torsion constant can be considered correct to three significant figures.

Although no current experimental tests were made, a comparison with earlier tests made by one of the authors is given in the first seven lines of Table 4. The present investigation did not disclose any great amount of error in the evaluation of α by the earlier soap film tests.[4] The average of the absolute values of the per cent variation tabulated in Column 5 of Table 4 for the seven earlier tests was 1.76 per cent for the currently proposed formulas for α as compared with 2.26 per cent for α values calculated by the results of the soap film tests. Thus

TABLE 4

COMPARISON BETWEEN COMPUTED TORSION CONSTANT J
AND PREVIOUS TEST RESULTS

(1)	(2)	(3)	(4)	(5)	(6)	(7)
		Torsion Constant J				
Test No.	Nominal Size	From Dimensions	By Test from Reference 3	Percentage Variation	$2 \alpha D^4$	$\frac{2 \alpha D^4}{J}$
T-14°	6WF20	.2408	.243	.9	.0277	.115
T-22°	8WF31	.4582	.451	- 1.6	.0645	.1407
T-25° x	10x12 (62)	1.989	1.960	- 1.5	.0839	.0421
T-26°	12I31.8	.817	.804	- 1.6	.0920	.1126
T-30°	12I55	3.290	3.380	2.7	.484	.1471
T-31°	12WF190	47.290	48.870	3.3	4.293	.0908
T-33°	12WF65	2.206	2.222	0.7	.246	.1115
Ship channel$*	6 In., 15.3 lb.	.211	.206	- 2.4	.0124	.0588
Heavy channel*	6 In., 15.5 lb.	.4249	.400	- 5.9	.0468	.1101
Standard channel*	10 In., 15.3 lb.	.216	.256	18.5	.01151	.0533
Standard channel*	15 In., 33.9 lb.	1.0229	1.08	5.6	.0606	.0592

°Test numbers used in Reference 3, which gives complete information on measured dimensions.

*Nominal dimensions are used, tests from Reference 12.

$Flange slope S = .0348.

xSection no longer manufactured.

there is improvement, most of which accrues from Test T-25, which was 6.7 per cent in error by the old formula.

In a discussion of Reference 3, Seeley and Putnam[12] reported on tests that they made of four channel sections and these are compared with the proposed channel shape formula in the last four lines of Table 4. The agreement is not particularly good, especially in the case of the 10 in., 15.3 lb. channel and the fact that the investigators used a shear modulus of 12,000 ksi in calculating their torsion constants indicates that the reported test values are lower than they should be. Seeley and Putnam point out that there was considerable deviation between the measured dimensions of the channel and the nominal or handbook dimensions but they used the nominal values and do not report the measured values. It is possible that the high value reported for the 10 inch channel is due to the fact that this channel might not have maintained its shape of cross-section during tests. The investigators measured only the angle of twist of the flange. Since this section has the thinnest web of any channels tested the actual twist of the web may have been greater than that of the individual flanges.

Seeley and Putnam correctly point out that the variation in their test results is greater than the variation between a more accurate evaluation of the torsion constant and the simple approximation

$$J = \sum \frac{bt^3}{3} \qquad (42)$$

They also correctly suggest that in using this equation neither the end loss correction nor juncture correction should be included since these two corrections tend to compensate. Including either correction without the other gives a poorer approximation than neglecting both.

The justification for the present evaluation of accurate formulas for channel and angles together with improvement in the earlier formulas for I beams and wide flange shapes is for the purpose of permitting more accurate evaluation for handbook listings. It is to be hoped that torsion constants will be listed in future steel handbooks as they provide a basis for the simplest and most accurate solution of problems involving combined torsion and bending as well as problems involving the lateral buckling of beams and columns made of I beam or WF shapes.

As indicated previously, the agreement between the formulas for angles with legs of equal thickness and experimental results obtained by Cullimore and Pugsley[9] is good, (Figure 12).

SUMMARY AND ACKNOWLEDGMENTS

This paper has provided a basis for the handbook tabulation of torsion constants for all currently manufactured hot rolled structural shapes with the exception of bulb angles and similar special shapes. Whereas such previous evaluation was necessarily made by means of soap film tests or by tedious desk calculator relaxation procedures, the advent of the digital computer has permitted the development of formulas of greater accuracy than hitherto was possible. Special acknowledgment is due the University of Michigan Computing Center facilities which permitted use of the many hours of computer time necessary for the many runs needed.

REFERENCES

1. Saint Venant, "Mémoire sur la Torsion des Prisimes, ..." Mémoires des Savants etrangers, 1855, T. XIV, pp. 233-560.

2. Prandtl, L. "Zür Torsion von Prismatischen Staben" Physikalische Zeitschrift, IV, 1903, p. 758.

3. Lyse, Inge, and Johnston, B. G. "Structural Beams in Torsion," Transactions of the Amer. Soc. of Civil Engineer, Vol. 101, 1936, p. 857.

4. Johnston, B. G. "Torsional Rigidity of Structural Sections," Civil Engineering Magazine, Nov. 1935, p. 698.

5. "Torsional Stresses in Structural Beams," Bethlehem Steel Co. Booklet, 1803.

6. Trayer, George W. and March, H. W. "The Torsion of Members Having Sections Common in Aircraft Construction," Technical Report of the Advisory Committee for Aeronautics, No. 334, 1930.

7. Christopherson, D. G. and Southwell, R. V. "Relaxation Methods Applied to Engineering Problems," Proc. Royal Soc., London, Series A, No. 934, Vol. 168, p. 317, Nov. 1938.

8. Shaw, F. S. "The Torsion of Solid and Hollow Prisms in the Elastic and Plastic Range by Relaxation Methods," Australian Council for Aeronautics. Report ACA-11, Nov. 1944.

9. Cullimore, M.S.G. and Pugsley, A.G. "The Torsion of Aluminum Alloy Structural Members," Research Report No. 9, The Aluminum Development Association, London, July, 1952.

10. Huth, J. H. "Torsional Stress Concentration in Angle and Square Tube Fillets," ASME Journal of Applied Mechanics, Vol. 17, No. 4, December, 1950.

11. Timoshenko, S. and Goodier, J. N. "Theory of Elasticity," McGraw-Hill, 1951.

12. Seely, F.B. and Putman, W. J. Discussion of Reference 3. Loc. Cit., pp. 907-912.

NOTATION

D_1, D_2, D_3, D_4	diameter of circle inscribed at juncture
F	a constant (a length)
G	shear modulus of elasticity
H	a constant (a length), network space
J	torsion constant
M_z	torsional moment
N	ratio of triangle base to mesh space
R	ratio of triangle altitude to mesh space
R_o	an arbitrary number
S	slope of flange
T	tension force per unit width in a membrane
V	volume under stress function surface
V, V_S, V_L	coefficient of end loss
b	overall breadth of flange
d	overall depth of section
p	pressure under a membrane
r	fillet radius
t, t_1, t_2, t_3	thickness of flange (See Figure 6)
x, y, z	coordinates
Θ	angle of twist per unit length
τ_{zx},τ_{zy},τ_{zr},τ_m	shear stress
α,α_1,α_2,α_3,α_4	coefficients of juncture correction to torsion constant
γ	coefficient for maximum shear stress in a rectangular cross-section
δ	coefficient of stress increase at tee juncture

ζ	z displacement of membrane
ϕ	dimensionless form of stress-function, ψ
ψ	torsion stress function
w	web thickness